Data in Brief 32 (2020) 106193

Contents lists available at ScienceDirect

Data in Brief

journal homepage: www.elsevier.com/locate/dib

Data Article

Data analysis for characterization of IG110 and A3 by X-Ray diffraction and Raman spectroscopy

Huali Wu[b,*], Ruchi Gakhar[c], Allen Chen[d], Zhou Zhou[e], Raluca O. Scarlat[a]

[a] Nuclear Engineering Department, University of California Berkeley, Berkeley, CA USA
[b] Department of Mechanical Engineering, Virginia Polytechnic Institute and State University, Blacksburg, VA USA
[c] Idaho National Laboratory, 2525 Fremont Ave., Idaho Falls, ID USA
[d] Department of Engineering Physics, University of Wisconsin-Madison, Madison WI USA
[e] School of Physics, Sun Yat-sen University, China

ARTICLE INFO

Article history:
Received 21 June 2020
Revised 12 August 2020
Accepted 13 August 2020
Available online 19 August 2020

Keywords:
Nuclear Graphite
IG110, A3
Crystallite edge area
XRD, Raman

ABSTRACT

This article contains data related to the research journal paper titled 'Comparative Analysis of Microstructure and Reactive Sites for Nuclear Graphite IG-110 and Graphite Matrix A3", *Journal of Nuclear Materials* 528 (2020) 151802. This article includes details of the calculation process of the crystallite edge area, additional tables and figures of XRD and Raman data, and additional summary of data reduction methods used in prior literature for the characterization of IG-110 nuclear graphite. Reduced data associated with this article is provided in the supplementary information. Raw data associated with this article is in the supplementary material of the companion article.

DOI of original article: 10.1016/j.jnucmat.2019.151802
* Corresponding Author.
E-mail address: huali@vt.edu (H. Wu).

https://doi.org/10.1016/j.dib.2020.106193

Specifications Table

Subject	Nuclear Energy and Engineering, Materials Science
Specific subject area	Graphite Microstructure and Chemical Reactivity
Type of data	Equations Tables Figures
How data were acquired	Raw data sets were acquired from X-ray diffraction (Bruker D8 Discover X-ray Diffractometer) and Raman Spectroscopy (Thermo Scientific DXR Raman microscope)
Data format	Secondary data of crystallite edge area, based on Raman and XRD data And Secondary data of microstructural parameters calculated from Raman and XRD data
Parameters for data collection	XRD and Raman data were all collected in air atmosphere, at room temperature. Graphite sample preparation details are provided in the companion article [13].
Description of data collection	XRD data was collected using 0.5 mm collimator in the 2θ range of 20^o to 90^o with an increment of 10^o. The scan time was 60 s. Raman Spectra were recorded with 200 exposures per spectrum and 0.5 s per exposure. The data was recorded at five arbitrary points on the surface of each sample.
Data source location	The raw XRD and Raman spectra, which were collected at University of Wisconsin-Madison, can be found in the Supplemental Information (SI) of the companion article [13].
Data accessibility	SI is provided with this *Data in Brief* article. The SI includes calculations and all analysed data from XRD and Raman spectra, and results of the CARBONX fitting of XRD spectra.
Related research article	Huali Wu, Ruchi Gakhar, Allen Chen, Stephen Lam, Craig P. Marshall and Raluca O. Scarlat Comparative Analysis of Microstructure and Reactive Sites for Nuclear Graphite IG-110 and Graphite Matrix A3 *Journal of Nuclear Materials* 528 (2020) 151802. doi:https://doi.org/10.1016/j.jnucmat.2019.151802

Value of the Data

- This article provides data that is instrumental in comparative analysis of two grades of nuclear graphite: IG-110 and A3.
- This article is useful for the researcher who wants to perform Raman and XRD analysis of graphite for characterization of microstructure, defects and reactive carbon sites, and who seeks to investigate sensitivity of the calculated microstructural parameters (d002, and La) to the data reduction method employed.
- Further comparative analysis can be performed between IG-110 and A3, based on the data sets provided here, for each of three faces of cubic samples of IG-110 and A3 analysed by XRD, and for five points on the surface of the samples analysed by Raman, and the data can be used for further comparisons of crystallite surface area contributions from different facets of crystallite surfaces.
- This article provides several data reduction methods for in-plane crystallite size (L_a) from Raman and out-of-plane lattice parameter (d_{002}) from XRD, and the calculated crystallite edge surface area along with the derivation of the equations used in this calculation.
- The multitude of data reduction methods used in the literature and reported here were the basis for selecting the data reduction approach that was used in the companion article [13].
- CarbonXS fitting of XRD data for IG110 and A3 is provided. Based on the results provided here, researchers can choose to perform additional CarbonXS fitting of the data for IG110 and A3, or draw conclusions about the necessity of CarbonXS fitting versus other methods of microstructural analysis based on the XRD spectrum.

1. Data Description

1.1. Estimation of Crystallite Edge Area

The edge area of graphite crystallites that is perpendicular to the graphene planes is calculated as follows. Two metrics of interest are computed: edge area per gram of graphite sample $\frac{A_{edge,\ cryst}}{m_{cryst}}$, and atomic ratio of edge carbons to total carbon atoms in a sample $\frac{C_{edge}}{C_{total}}$.

$$A_{edge,\ cryst} = P_{top}\ L_c \tag{1}$$

where $A_{edge,\ cryst}$ is the surface area of the crystallite edge (surface perpendicular to the graphene layers), P_{top} is the perimeter of the crystallite top (surface parallel to the graphene layers), ρ_{cryst} is the density of one crystallite, V_{cryst} is the volume of the one crystallite, $m_{cryst} = V_{cryst}\ \rho_{cryst} = A_{top}\ L_c\ \rho_{cryst}$ is the mass of the crystallite, and A_{top} is the surface of the crystallite top (surface parallel to the graphene layers).

Assumptions:

1 $\frac{P_{top}}{A_{top}} = \frac{4}{L_a}$, which is valid for circle, square, and hexagonal shape.
2 The density of a perfect graphite crystallite is used; $\rho_{cryst} = 2.266\ \frac{g}{cm^3} = 2.266\ E-21\ g/nm^3$ for perfect graphite with c = 0.670, and a = 0.246 nm. The actual crystallite density is proportional to $a^2 \cdot c$; therefore the assumption of a perfect crystal density introduces an error of less than 1%.

Incorporating the two assumptions above, we obtain the following expressions for specific crystallite edge surface area.

$$\frac{A_{edge,\ cryst}}{m_{cryst}} = \frac{P_{top}\ L_c}{A_{top}\ L_c\ \rho_{cryst}} = \frac{P_{top}}{\rho_{cryst}\ A_{top}} = \frac{4}{\rho_{cryst}\ L_a} \tag{2}$$

$$\frac{A_{edge,\ cryst}}{m_{cryst}} = \frac{1770}{L_a[nm]} \left[\frac{m^2}{g}\right] \tag{3}$$

The number of edge carbon atoms can be estimated similarly to the estimation of edge surface area.

$$N_{edge} = N_{C,perimeter}\ N_{layers} \tag{4}$$

where N_{edge} is the number of atoms on the edge of a crystallite, $N_{C,\ perimeter}$ is the number of atoms on the edge of one graphene layer inside a crystallite, N_{layers} is the number of graphene layers in a crystallite.

$$N_{layers} = 2\frac{L_c}{c} \tag{5}$$

$$N_{C,perimeter} = N_{arm-chair\ sides} + N_{zig-zag\ sides} \tag{6}$$

where $N_{arm-chair\ sides}$ is the number of atoms on the armchair edges of a graphene sheet, $N_{arm-chair\ sides}$ is the number of atoms on the zig-zag edges of a graphene sheet

$$N_{arm-chair\ sides} = \frac{2 \cdot 4 \cdot L_a}{3a/\sqrt{3}} = 4.62\ \frac{L_a}{a} \text{ (derived approximating to a square graphene sheet)} \tag{7}$$

$$N_{zig-zag\ sides} = 2 \cdot 2 \cdot \frac{L_a}{a} \text{ (derived approximating to a square graphene sheet)} \tag{8}$$

$$N_{C,perimeter} = \left(4 + \frac{8}{\sqrt{3}}\right) \frac{L_a}{a} = 8.62\ \frac{L_a}{a} \tag{9}$$

$$N_{edge} = 17.24\ \frac{L_c}{c}\ \frac{L_a}{a} \tag{10}$$

$$N_{cryst} = \frac{V_{cryst}\ \rho_{cryst}}{12\left(\frac{g}{mol}\right)}\ N_A\left(\frac{at}{mol}\right) \tag{11}$$

where N_{cryst} is the number of atoms in a crystallite, N_A is Avogadro's number

$$V_{cryst} = A_{top}\ L_c = L_a^2\ L_c \text{ (derived approximating to a square graphene sheet)} \tag{12}$$

$$N_{cryst} = \frac{L_a^2\ L_c\ \rho_{cryst}}{12\left(\frac{g}{mol}\right)}\ N_A\left(\frac{at}{mol}\right) \tag{13}$$

$$\frac{\boldsymbol{N_{edge}}}{\boldsymbol{N_{cryst}}} = \frac{17.24\ \frac{\boldsymbol{L_c}}{\boldsymbol{c}}\ \frac{\boldsymbol{L_a}}{\boldsymbol{a}}}{L_a^2\ L_c\left[1e-21\left(\frac{cm^3}{nm^3}\right)\right]}\ \frac{12\left(\frac{g}{mol}\right)}{\rho_{cryst}\ 6.022E23\left(\frac{at}{mol}\right)} = \frac{34E-23\left(\frac{g}{at}\right)}{\rho_{cryst}}\ \frac{1}{c\ a\ L_a} \tag{14}$$

$$\frac{\boldsymbol{C_{edge}}}{\boldsymbol{C_{total}}} = \frac{\boldsymbol{N_{edge}}}{\boldsymbol{N_{cryst}}} = \frac{0.15\ \left(nm^3\right)}{c\ a\ L_a} \tag{15}$$

where C_{edge} is the total number of carbon atoms located on the edge of crystallites, C_{total} is the total number of carbon atoms that comprise the crystallites.

Table 1 provides $\boldsymbol{C_{edge}/C_{total}}$ calculated for IG110 and A3, based on microstructural parameters estimated from XRD and Raman.

1.2. Raman Analysis: In-plane L_a crystallite size

Table 2 gives the L_a values calculated based on the several empirical equations available in the literature for estimating crystallite size L_a. Empirical correlations relate the Raman spectra (the peak maximum or area or FWHM of D and G bands) to L_a calculated from XRD and scanning tunneling microscopy, valid across different types of graphite materials. Tuinstra and Koening proposed Eqn. 16 with C(λ) = 4.4 nm, which is only valid for λ = 514.5nm. I_D and I_G are calculated as peak area [1].

$$\boldsymbol{L_a(nm)} = \boldsymbol{C(\lambda)}\left(\frac{\boldsymbol{I_D}}{\boldsymbol{I_G}}\right)^{-1} \tag{16}$$

Zheng et. al. [2] performs L_a calculations based on maximum peak intensity. Maslova et al. proposed the relationship between FWHM of G band and L_a in Eqn. 17, based on Ammar's research on polished samples [3,4], which holds for any excitation laser energy in the visible range:

$$\boldsymbol{L_a(nm)} = \frac{430}{\boldsymbol{FWHM(G)} - 14} \tag{17}$$

where 14 is the FWHM(G) for highly oriented pyrolytic graphite for which the D band is missing [5]. Table 2 provides the analyzed data for all sampled points on the surface of A3 and IG-110 and the corresponding L_a values from each of the available empirical correlations.

1.3. XRD Analysis

Fig. 1 provides an overlay of raw XRD data for three orthogonal faces of IG-110 and A3.

Table 1
Content of edge carbon in IG110 and A3, calculated from Eqn. 15 based on *c from XRD and L_a from XRD* and Raman. XRD a_{112} *is used for all calculations.*

	C_{edge}/C_{total} for IG110			C_{edge}/C_{total} for A3		
	$c_{Cryst.1}$	$c_{Cryst.2}$	c	$c_{Cryst.1}$	$c_{Cryst.2}$	c
$L_{a,\ XRD}$	0.0428 ± 0.0163	0.0431 ± 0.0164	0.0430 ± 0.0164	0.0390 ± 0.0025	0.0392 ± 0.0025	0.0392 ± 0.0025
$L_{a,\ Raman}$	0.0272 ± 0.0074	0.0274 ± 0.0075	0.0274 ± 0.0075	0.0265 ± 0.0093	0.0266 ± 0.0094	0.0266 ± 0.0094
	H/C_{edge} at 10 kPa H_2 and 700°C, for IG110			H/C_{edge} at 10 kPa H_2 and 700°C, for A3		
$L_{a,\ XRD}$	561 ± 284	557 ± 282	558 ± 282	2309 ± 209	2296 ± 208	2296 ± 208
$L_{a,\ Raman}$	881 ± 380	876 ± 377	877 ± 378	3399 ± 440	3380 ± 438	3379 ± 437
	$A_{edge,cryst}/m_{cryst}$ for IG110			$A_{edge,cryst}/m_{cryst}$ for A3		
$L_{a,\ XRD\ (101)}$	84 ± 32			77 ± 5		
$L_{a,\ Raman}$	54 ± 12			52 ± 18		

Table 2
FWHM and L_a for IG-110 and A3 Graphite

Graphite	Point[1]	FWHM (cm^{-1})		I_D/I_G	L_a _Eqn. 16	L_a _ Eqn. 17	I_D/I_G	L_a _ Eqn. 16	L_a _ Eqn. 17
		D	G	(area ratio)	(nm)		(Intensity ratio)		
A3	Point 1	55.3	26.3	0.78	6	35	0.38	12	35
	Point 2	54.1	23.0	0.57	8	48	0.24	18	48
	Point 3	53.5	26.3	0.77	6	35	0.38	12	35
	Point 4	55.5	27.3	0.31	14	32	0.14	31	32
	Point 5	52.6	24.6	0.74	6	41	0.35	13	41
	Average	54.2	25.5	0.64	8	38	0.30	17	38
	σ	1.0	1.5	0.18	3	5	0.09	7	5
IG-110	Point 1	42	23.4	0.75	6	46	0.42	10	46
	Point 2	46	24.7	0.79	6	40	0.42	11	40
	Point 3	46	24.6	0.49	9	40	0.27	17	40
	Point 4	47	21.6	0.40	11	56	0.20	22	56
	Point 5	49	26.8	0.74	6	34	0.39	11	34
	Average	46	24.2	0.63	8	43	0.34	14	43
	σ	2	1.7	0.16	2	8	0.09	5	8
Confidence level (A3 ≠ IG-110)		99.9%	70.0%	0.0%	0.0%	0.0%	10.0%	10%	10%
IG-110[2]				0.34(10) [2]					62(23)
IG-110 Zheng et.al[2],[3]				0.51(10) [2],[3]					39(7)

[1] The Raman spectrometer samples points on the surface of graphite of approximately 1 micrometer in diameter.
[2] I_D/I_G and L_a calculated based on D and G peak maximum intensity.
[3] Standard deviation based on spectra at three points on the graphite surface.

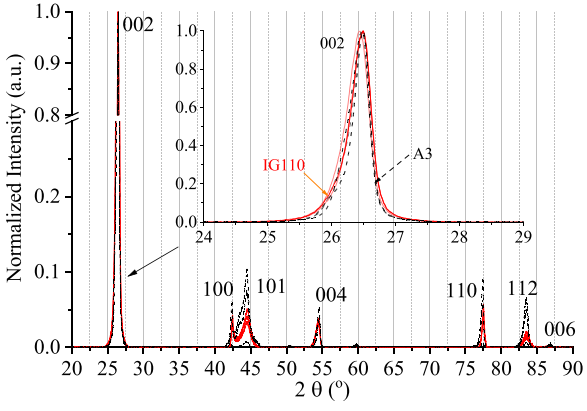

Figure 1. Comparison of XRD patterns of IG-110 graphite (orange solid lines) and A3 (blue dashed lines). Patterns from three orthogonal faces from each sample are shown.

Table 3
Interlayer spacing and degree of graphitization from XRD, using different approaches for determining d_{002}.

		[1]d_{002}(nm)	[1]$\bar{g}$	[2]d_{002}(nm)	[3]d_{002}(nm)
IG-110	Cryst. 1	0.3389(3)	60(7)	0.3391(10)	0.3373(4)
	Cryst. 2	0.3367(3)	84(4)	0.3371(2)	
IG-110 Powder	Cryst. 1	0.3387(14)	62(16)	(extrapolation method does not apply)	
	Cryst. 2	0.3365(1)	84(6)		
A3	Cryst. 1	0.3384(4)	65(5)	0.3380(9)	0.3364(2)
	Cryst. 2	0.3365(1)	88(2)	0.3365(3)	

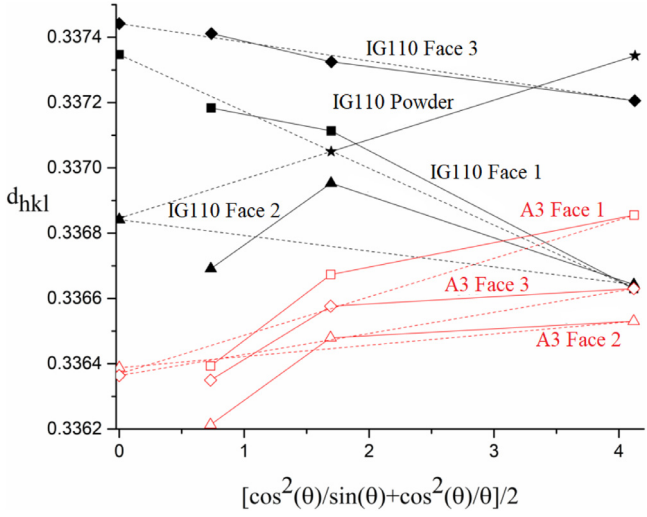

Figure 2. Determination of ${}^{3}d_{002}$ parameter based on θ_{002}, θ_{004}, θ_{006} peaks

Table 4
In-plane lattice parameter *a* for IG-110 and A3, without peak deconvolution. Peak maxima is used for computing a from (101), (100), (110), and (112) reflections.

	a_{ave} (nm)
IG-110	0.2463(2)
A3	0.2461(4)
IG-110 Powder	0.251(6)

1.3.1. Out of plane lattice parameter d_{002}

Table 3 provides the values of d_{002} calculated with three different calculation approaches, ${}^{1}d_{002,}$ ${}^{2}d_{002,}$ and ${}^{3}d_{002}$:

- ${}^{1}d_{002}$ is an average of (002) and (004) reflection calculations from Bragg's law; the standard deviation across the two reflections and three faces is reported.
- ${}^{2}d_{002}$ and 3d002 use the extrapolation method that takes into account x-ray absorption effects and instrumental setup [6,7]. For the powder IG-110 sample, the extrapolation method is not applicable because the sample thickness was less than 1 mm and X-ray penetration depth is larger than 5 mm.
- ${}^{2}d_{002}$ uses peaks (002) and (004) of the deconvoluted data that assumed two crystallite groups. The standard deviation across the three faces is reported in Table 3.
- ${}^{3}d_{002}$ uses non-peak fitted data (maximum value of the single peak), and hence assumes a single crystallite group. The d002 extrapolation from all (00x) peaks for each of the samples is shown in Fig. 1. The standard deviation across the three faces is reported in Table 3.

1.3.2. In-plane lattice parameter a

Table 4 provides the calculated in-place lattice parameter *a*. Averaged lattice parameters without peak deconvolution (i.e. utilizing the location of the peak maximum) are reported, using the calculation methodology reported in [2,9–11]. The standard deviation across the three faces and four reflections is reported in Table 4. Averaged *a* calculated from peak-fitted XRD data were reported in the companion article [13].

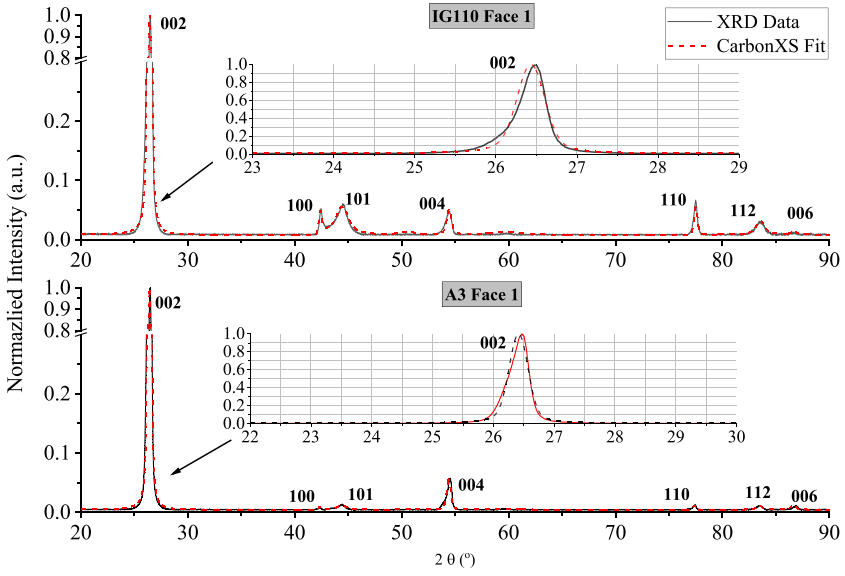

Figure 3. CarbonXS fitting results of Face 1 of IG110 and A3 sample

Table 5
Parameters calculated from CarbonXS for IG110 and A3, and comparison with prior microstructural analysis

	IG110	A3	IG110 vs. A3	Same Conclusion with:
a	2.461499(1)	2.464806(7)	<	XRD PF Analysis
La	266.1(1)	308.8(8)	<	XRD PF Analysis
$P_{Random\ staking}$	0.14688(9)	0.0671(6)	>	Raman G'_2D
$P_{3R\ staking}$	0.08195(7)	0.1031(1)	<	XRD 3R Analysis
Preferred Orientation Factor	-0.0691(6)	2.1943(8)	<	XRD Bacon Factor

1.3.3. CarbonXS Peak Fitting Data

The XRD pattern of IG110 and A3 was fitted with CarbonXS, which is a XRD fitting software especially design for graphite [2,8,12]. A constant background was used, and the second layer model was used because both IG110 and A3 have quite high graphitization. CARBONXS does not account for the instrument resolution. CarbonXS performs peak fitting and accounts for certain types of layer misalignment defects in the graphite crystallites and for crystallite strain; the software does not account for non-Gaussian crystallite population distributions. Section 1.3.3 provides results of CarbonXS fitting. Fig.3 shows the fitting results. Asymmetry of the peaks cannot be fully reproduced. Table 5 shows the calculated microstructural parameters.

2. Experimental Design, Materials, and Methods

Two types of carbon materials were characterized with XRD and Raman Spectroscopy: nuclear graphite IG110 and graphite matrix A3. IG-110 was provided by the MIT Nuclear Reactor Laboratory and the material was originally procured from Toyo Tanso Co. Japan and A3 cylindrical compacts were prepared by Oak Ridge National Laboratory (ORNL). XRD patterns were collected using a Bruker D8 Discover X-ray Diffractometer, using Cu radiation ($K\alpha = 0.15418$ nm).

Raman Spectra were recorded using a Thermo Scientific DXR Raman microscope operated with a 532 nm laser. Both XRD and Raman spectra diffraction patterns were normalized to unity intensity for the highest-intensity peak. Peak fitting was done with PeakFit v4 software using Voigt functions, which are a combination of Gaussian and Lorentzian functions. Detailed description of materials, data collection and data analyzing methods can be found in the companion article [13].

3. Contributions

H.W. proposed and performed the sample preparation, R.G. and A.C. performed the XRD and Raman measurements; H.W. proposed and performed the XRD and Raman peak fitting analysis; R. S. proposed and performed the numerical calculation of crystallite edge area. Z.Z. performed the XRD fitting analysis with CARBONX. H.W., R.G., and A.C. analyzed the data and performed the error analysis. H.W. and R.S. wrote the paper.

Declaration of Competing Interest

None.

Acknowledgements

This work was supported by U.S. DOE NEUP grants 15-8352 and IRPDE-NE0008285, and U.S. NRC Grant NRC-HQ-84-15-G-0046. Instrumentation support at the UW Materials Research Science and Engineering Center was provided by NSF Grant DMR-1121288 for XRD facilities and DMR-1121288, 0079983 and 0520057 and for Raman analysis. Authors thank Tim Burchell, Cristian Contescu and Michael P. Trammell at ORNL and Lin-wen Hu, David Carpenter and Tony Zheng at the MIT Nuclear Reactor for providing graphite samples and information about the manufacturing process, and Gabriel Meric de Bellefon at University of Wisconsin-Madison for discussion of XRD analysis.

Supplementary materials

Supplementary material associated with this article can be found, in the online version, at doi:10.1016/j.dib.2020.106193.

References

[1] F. Tuinstra, L. Koenig, Raman Spectrum of Graphite, J. Chem. Phys. 53 (1970) (1970) 1126–1130 https://doi.org/10.1063/1.1674108.
[2] G. Zheng, P. Xu, et al., Characterization of structural defects in nuclear graphite IG-110 and NBG-18, J. Nucl. Mater. 446 (1–3) (2014) 193–199 https://doi.org/10.1016/j.jnucmat.2013.12.013.
[3] M.R. Ammar, J.N. Rouzaud, How to obtain a reliable structural characterization of polished graphitized carbons by Raman microspectroscopy, J. Raman Spectrosc. 43 (2) (2012) 207–211 https://doi.org/10.1002/jrs.3014.
[4] M.R. Ammar, E. Charon, et al., On a reliable structural characterization of polished carbons in meteorites by Raman microspectroscopy, Spectrosc. Lett. 44 (7–8) (2011) 535–538 http://dx.doi.org/10.1080/00387010.2011.610417.
[5] O.A. Maslova, M.R. Ammar, et al., Determination of crystallite size in polished graphitized carbon by Raman spectroscopy, Phys. Rev. B - Condens. Matter Mater. Phys. 86 (13) (2012) 1–5 http://dx.doi.org/10.1103/PhysRevB.86.134205.
[6] M.S. Seehra, A.S. Pavlovic, et al., X-Ray Diffraction, Thermal Expansion, Electrical Conductivity, and Optical Microscopy Studies of Coal-Based Graphites, Carbon N. Y. 31 (4) (1993) 557–564 https://doi.org/10.1016/0008-6223(93)90109-N.
[7] J.B. Nelson, D.P. Riley, An experimental investigation of extrapolation methods in the derivation of accurate unit-cell dimensions of crystals, Proc. Phys. Soc. 57 (3) (1945) 160–177 http://dx.doi.org/10.1088/0959-5309/57/3/302.

[8] Z. Zhou, W.G. Bouwman, et al., Interpretation of X-ray diffraction patterns of (nuclear) graphite, Carbon N. Y. 69 (2014) 17–24 https://doi.org/10.1016/j.carbon.2013.11.032.
[9] D.J. Kim, H. Jang, et al., X-Ray Diffraction Measurements of Ion-Irradiated Graphite, Int. Nucl. Inf. Syst. 17 (17) (2005) 1–2.
[10] Z.Q. Li, C.J. Lu, et al., X-ray diffraction patterns of graphite and turbostratic carbon, Carbon 45 (8) (2007) 1686–1695 https://doi.org/10.1016/j.carbon.2007.03.038.
[11] S.H. Chi, G.C. Kim, Comparison of the oxidation rate and degree of graphitization of selected IG and NBG nuclear graphite grades, J. Nucl. Mater. 381 (1–2) (2008) 9–14 https://doi.org/10.1016/j.jnucmat.2008.07.027.
[12] Lok-kun Tsui, Fernando Garzon, CarbonXS GUI: a graphical fron-end for CarbonXS, J. Appl. Cryst. 50 (2017) 1830–1833 https://doi.org/10.1107/S1600576717015035.
[13] Huali Wu, Ruchi Gakhar, Allen Chen, Stephen Lam, Craig P. Marshall, Raluca O. Scarlat, Comparative analysis of microstructure and reactive sites for nuclear graphite IG-110 and graphite matrix A3, Journal of Nuclear Materials 528 (2020) 151802 https://doi.org/10.1016/j.jnucmat.2019.151802.